Correction of depolarization effect in Mueller matrix ellipsometry with polar decomposition method

Weiqi Li [1], Chuanwei Zhang [1,2], Hao Jiang [1], Xiuguo Chen [1], Honggang Gu [1], and Shiyuan Liu [1,2,*]

[1] *State Key Laboratory of Digital Manufacturing Equipment and Technology, Huazhong University of Science and Technology, Wuhan 430074, China*

[2] *Wuhan Eoptics Technology Co., Ltd., Wuhan 430075, China*

ABSTRACT

Mueller matrix ellipsometry has been demonstrated as a powerful tool for nanostructure metrology in high-volume manufacturing. Many factors may induce depolarization effect in the Mueller matrix measurement, and consequently, may lead to accuracy loss in the nanostructure metrology. In this paper, we propose to apply a Mueller matrix decomposition method for the Mueller matrix measurement to separate the depolarization effect caused by the MME system. The method is based on the polar decomposition by decomposing the measured depolarizing Mueller matrix into a sequence of three matrices corresponding to a diattenuator followed by a retarder and a depolarizer. Since the depolarization effects will be only reflected in the depolarizer matrix, the other two matrices are used to extract the structure parameters of the measured sample. Experiments performed on a one-dimensional silicon grating structure with an in-house developed MME layout have demonstrated that the proposed method achieves a higher accuracy in the nanostructure metrology.

Keywords: Mueller matrix ellipsometry (MME); nanostructure metrology; depolarization effect; polar decomposition.

1. INTRODUCTION

Ellipsometry is an optical metrology technique that utilizes polarized light to characterize thickness of thin films and optical constants of both layered and bulk materials [1]. Since the year of around 2000, spectroscopic ellipsometry (SE) was introduced to monitor the critical dimension (CD) of grating structures in semiconductor manufacturing [2-4]. Compared with scanning electron microscopy (SEM), atomic force microscopy (AFM), or transmission electron microscopy (TEM), this technique, sometimes also referred to as optical scatterometry or optical critical dimension metrology, has achieved wide industrial applications due to its attractive advantages, such as low cost, high throughput, and minimal sample damage [5,6]. Among the various types of ellipsometers, Mueller matrix ellipsometer (MME) can provide all 16 elements of the 4 by 4 Mueller matrix in each measurement. Compared with conventional ellipsometer, which at most obtains two ellipsometric angles, MME can acquire much more useful information about the sample, such as anisotropy and depolarization. Therefore, MME is expected to be a powerful tool for nanostructure metrology in high-volume nanomanufacturing [7].

One of the critical procedures in MME is to acquire the accurate Mueller matrix spectrum of the sample. Many factors may induce depolarization effect in the Mueller matrix measurement, and consequently, may lead to accuracy loss in the nanostructure metrology. Some factors are rising from the MME system and cannot be avoided, such as the finite spectral bandwidth of the monochromator and detector, the finite numerical aperture (NA) of the focusing lens. Germer and Patrick consider the effects of finite bandwidth and NA on the theoretical simulations. Since the incidence angle and the azimuthal angle are varied with the whole exit pupil of the focus lens, and the wavelength will vary over the bandwidth range, they proposed an efficient integration methods based upon Gaussian quadrature in one dimension for spectral bandwidth averaging and two dimensions inside a circle for numerical aperture averaging to investigate the effects of finite bandwidth and NA [8]. After that, the depolarization effects caused by the finite bandwidth and NA are considered, and incorporated into the optical model of the measured structure [9, 10]. However, this integration method which needs to calculated the Mueller matrices dozens of times, is extraordinarily time consuming, since the Mueller

* Corresponding author: shyliu@hust.edu.cn; phone: +86 27 8755 9543; webpage: http://www2.hust.edu.cn/nom .

Modeling Aspects in Optical Metrology V, edited by Bernd Bodermann, Karsten Frenner, Richard M. Silver,
Proc. of SPIE Vol. 9526, 952619 · © 2015 SPIE · CCC code: 0277-786X/15/$18 · doi: 10.1117/12.2184786

matrix calculation method, such as the rigorous couple-wave analysis (RCWA) [11-13], finite-difference time-domain (FDTD) method [14], or finite element method (FEM) [15, 16] are always complex and time-consuming. In this paper, we propose to apply a Mueller matrix decomposition method for the Mueller matrix measurement to separate the depolarization effect caused by the MME system. The method is based on the polar decomposition by decomposing the measured depolarizing Mueller matrix into a sequence of three matrices corresponding to a diattenuator followed by a retarder and a depolarizer [17]. The depolarization effects mainly induced by the MME system will be only reflected in the depolarizer matrix. Therefore, we may only use the other two matrices for the structure parameter reconstructions to exclude the depolarization effects from the measurement. We performed experiments on the Si gratings with an in-house developed dual rotating-compensator MME prototype, and expected higher measurement accuracy is achieved.

2. METHOD

2.1 Polar decomposition

Polar decomposition consists of decomposing an arbitrary Mueller matrix $\mathbf{M}$ into the product of three elementary matrices representing a retarder $\mathbf{M}_R$, a diattenuator $\mathbf{M}_D$, and a depolarizer $\mathbf{M}_\Delta$. Because of the noncommutativity of the matrix product, the decomposition leads to the existence of six possible products [18]:

$$\begin{aligned}\mathbf{M} = \{&\mathbf{M}_{\Delta 1}\mathbf{M}_{R1}\mathbf{M}_{D1}, \quad \mathbf{M}_{\Delta 2}\mathbf{M}_{D2}\mathbf{M}_{R2}, \quad \mathbf{M}_{R3}\mathbf{M}_{\Delta 3}\mathbf{M}_{D3}, \\ &\mathbf{M}_{D4}\mathbf{M}_{R4}\mathbf{M}_{\Delta 4}, \quad \mathbf{M}_{R5}\mathbf{M}_{D5}\mathbf{M}_{\Delta 5}, \quad \mathbf{M}_{D6}\mathbf{M}_{\Delta 6}\mathbf{M}_{R6}\}.\end{aligned} \tag{1}$$

According to the order of the diattenuator and the depolarizer matrices in the products, these six products can be divided into two families, namely the forward family and the reverse family [19]. In particular, the forward family physically corresponds to the depolarizer being in front of the diattenuator expressed as:

$$\mathbf{M} = \mathbf{M}_\Delta \mathbf{M}_R \mathbf{M}_D, \tag{2a}$$

$$\mathbf{M} = \mathbf{M}_\Delta \mathbf{M}'_D \mathbf{M}_R, \tag{2b}$$

$$\mathbf{M} = \mathbf{M}_R \mathbf{M}'_\Delta \mathbf{M}_D, \tag{2c}$$

while the reverse family corresponds to the depolarizer being behind the diattenuator described by:

$$\mathbf{M} = \mathbf{M}_D \mathbf{M}_R \mathbf{M}_\Delta, \tag{3a}$$

$$\mathbf{M} = \mathbf{M}_R \mathbf{M}''_D \mathbf{M}_\Delta, \tag{3b}$$

$$\mathbf{M} = \mathbf{M}_D \mathbf{M}''_\Delta \mathbf{M}_R. \tag{3c}$$

The members within each family can be equivalent to one another under the following orthogonal transformations generated by the retarder matrix $\mathbf{M}_R$:

$$\mathbf{M}'_D = \mathbf{M}_R \mathbf{M}_D \mathbf{M}_R^T, \tag{4a}$$

$$\mathbf{M}'_\Delta = \mathbf{M}_R^T \mathbf{M}_\Delta \mathbf{M}_R, \tag{4b}$$

$$\mathbf{M}''_D = \mathbf{M}_R^T \mathbf{M}_D \mathbf{M}_R, \tag{4c}$$

$$\mathbf{M}''_\Delta = \mathbf{M}_R \mathbf{M}_\Delta \mathbf{M}_R^T. \tag{4d}$$

Morio and Goudail demonstrated that the forward family always leads to physical elementary Mueller matrices, whereas the other family does not [18]. Thus the forward polar decomposition is used in this paper, and the decomposition (2a) is considered as the normal forms of forward family due to the transformation properties.
According to work reported by Lu and Chipman [17], an m_{11} normalized Mueller matrix $\mathbf{M}$ can be rewritten as:

$$\mathbf{M} = \begin{bmatrix} 1 & \vec{D}^T \\ \vec{P} & \mathbf{m} \end{bmatrix}, \tag{5}$$

where $\vec{D}$ and $\vec{P}$ are the diattenuation and polarizance vectors of **M**, and **m** is a 3 by 3 matrix obtained by striking out the first row and the first column of **M**. In the polar decompositions (2a), the diattenuator $\mathbf{M}_D$ is a symmetric matrix and given by:

$$\mathbf{M}_D = \begin{bmatrix} 1 & \vec{D}^T \\ \vec{D} & \mathbf{m}_D \end{bmatrix}, \tag{6a}$$

$$\mathbf{m}_D = \left(1-D^2\right)^{1/2}\mathbf{I} + \left[1-\left(1-D^2\right)^{1/2}\right]\overrightarrow{D_u}\,\overrightarrow{D_u}^T, \tag{6b}$$

where **I** is the 3 by 3 identity matrix, D is the length of the diattenuation vector $\vec{D}$, and $\overrightarrow{D_u}$ denotes the unit vector along $\vec{D}$. The retarder $\mathbf{M}_R$ is represent by orthogonal matrix

$$\mathbf{M}_R = \begin{bmatrix} 1 & \vec{0}^T \\ \vec{0} & \mathbf{m}_R \end{bmatrix}, \quad \mathbf{m}_R^T = \mathbf{m}_R^{-1}, \tag{7}$$

while the depolarizer $\mathbf{M}_\Delta$ is defined as:

$$\mathbf{M}_\Delta = \begin{bmatrix} 1 & \vec{0}^T \\ \vec{P} & \mathbf{m}_\Delta \end{bmatrix}, \quad \mathbf{m}_\Delta^T = \mathbf{m}_\Delta. \tag{8}$$

2.2 Correction method

When a sample has the depolarization effect, totally polarized light used as a probe in ellipsometry is transformed into partially polarized light after the interactions with the sample, and the associated Mueller matrix will become a depolarizing one. The depolarization effect can be described by the depolarization index *DI* that is defined by [20]:

$$DI = \left[\frac{Tr\left(\overline{\mathbf{M}}\,\overline{\mathbf{M}}^T\right) - m_{11}^2}{3m_{11}^2}\right]^{1/2}, \quad 0 \le DI \le 1, \tag{9}$$

where m_{11} is the (1, 1)th element of the Mueller matrix **M**, $\mathbf{M}^T$ is the transposed matrix of **M**, and $\mathrm{Tr}(\cdot)$ represents the trace. *DI* = 0 and *DI* = 1 correspond to a totally depolarizing and non-depolarizing Mueller matrix, respectively. Many factors will induce depolarization effects and these factors can be classified overall into two categories, namely, the extrinsic and intrinsic causes [9]. The intrinsic causes include those that are closely related with the measured sample such as thickness nonuniformity, large surface or edge roughness, and thick transparent substrates. The extrinsic causes which are always accompanied with the MME system, such as the finite bandwidth of the monochromator and detector, and the finite numerical apertures of the focusing lens, will induce depolarization effects in the measurement process.

When performing the polar decomposition on the sample Mueller matrix, the depolarization effects will be only reflected in the depolarizer matrix. In case the depolarization effects are introduced by the MME system, we may simply use the other two matrices to extract the structure of the measured sample. A least-squares regression analysis (Levenberg-Marquardt algorithm) is performed, in which the model parameters are varied until calculated and experimental data match as much close as possible [21]. This is done by minimizing a mean square error function χ^2 defined by:

$$\chi^2 = \frac{1}{15N-P}\sum_{\lambda=1}^{N}\sum_{i,j=1}^{4}\left\{\left[(m_{ij,\lambda}^m)_D - (m_{ij,\lambda}^c)_D\right]^2 + \left[(m_{ij,\lambda}^m)_R - (m_{ij,\lambda}^c)_R\right]^2\right\}, \tag{10}$$

where λ denotes the spectral point from the total number *N* and *P* denotes the total number of the fitting parameters. $(m_{ij,\lambda}^m)_D$ and $(m_{ij,\lambda}^m)_R$ are the element of the diattenuator and retarder matrix decomposed from the measured Mueller matrix with the λth wavelength, respectively, and $(m_{ij,\lambda}^c)_D$ and $(m_{ij,\lambda}^c)_R$ are the corresponding diattenuator and

retarder matrix elements obtained from the calculation Mueller matrix. Indices i and j show all the matrix elements except m_{11}. As a theoretical reference, the Mueller matrix of the silicon grating can be calculated by the RCWA.

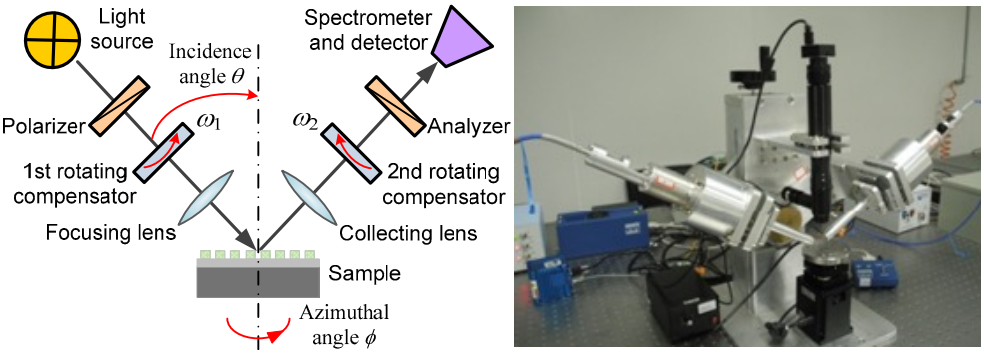

Figure 1. Principle and prototype of the dual rotating-compensator Mueller matrix ellipsometer.

3. EXPERIMENTS

3.1 Experiment setup

As schematically shown in Fig. 1, the basic system layout of the DRC MME in order of light propagation is $PC_{r1}(\omega_1)SC_{r2}(\omega_2)A$, where P and A stand for the polarizer and analyzer, C_{r1} and C_{r2} refer to the 1st and 2nd rotating compensators, and S stands for the sample. The fast axis angle C_1 and C_2 of the 1st and 2nd compensators rotate synchronously at $\omega_1 = 5\omega$ and $\omega_2 = 3\omega$, where ω is the fundamental mechanical frequency. The emerging Stokes vector $\mathbf{S}_{out}$ of the exiting light beam can be expressed as the following Mueller matrix product [22]:

$$\mathbf{S}_{out} = [\mathbf{M}_A\mathbf{R}(A)]\left[\mathbf{R}(-C_2)\mathbf{M}_{C_2}(\delta_2)\mathbf{R}(C_2)\right]\times\mathbf{M}_S\times\left[\mathbf{R}(-C_1)\mathbf{M}_{C_1}(\delta_1)\mathbf{R}(C_1)\right][\mathbf{R}(-P)\mathbf{M}_P\mathbf{R}(P)]\mathbf{S}_{in}, \quad (11)$$

where $\mathbf{M}_i$ (i = P, A, C_1, C_2) is the Mueller matrix associated with each optical element. $\mathbf{R}(\alpha)$ is the Mueller rotation transformation matrix for rotation by the angle α ($\alpha = P, A, C_1, C_2$) that describes the corresponding orientation angle of each optical element. δ_1 and δ_2 are the wavelength-dependent phase retardances of the 1st and 2nd rotating compensators. By multiplying the matrices in Eq. (11), we can obtain the following expression for the irradiance at the detector (proportional to the first element of $\mathbf{S}_{out}$) [7, 22]:

$$I(t) = I_0\left\{1+\sum_{n=1}^{16}\left[\alpha_{2n}\cos(2n\omega t-\phi_{2n})+\beta_{2n}\sin(2n\omega t-\phi_{2n})\right]\right\}, \quad (12)$$

where I_0, α_{2n} and β_{2n} are the d.c. and d.c-nomalized a.c. harmonic coefficients, respectively. The sample Mueller matrix elements M_{ij} (i, j = 1, 2, 3, 4) are linear combinations of α_{2n} and β_{2n}. By performing Fourier analysis [21], the Mueller matrix elements of the sample can be extracted from these harmonic coefficients. Based on the above measurement principle, we developed a DRC MME prototype. The spectral range is from 200 to 1000 nm. The beam diameter can be changed from the nominal value of ~3 mm to a value of ~200 μm equipped with the focusing lens. The two arms of the ellipsometer and the sample stage can be rotated to change the incidence and azimuthal angles in experiments.

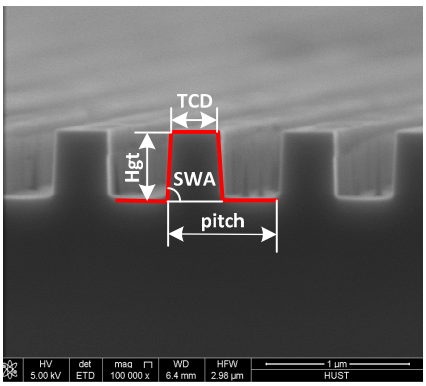

Figure 2. SEM cross-section image of the investigated Si grating.

The investigated sample is a one-dimensional Si grating, whose scanning electron microscope (SEM) cross-section image is shown in Fig. 2. The etched Si grating is chosen for this study due to its long-term dimensional stability, higher refractive index contrast, and relevance to the semiconductor industry. Optical properties of Si are taken from Ref. [23]. As depicted in Fig. 2, a cross-section of the Si grating is characterized by a symmetrical trapezoidal model with top critical dimension *TCD*, grating height *Hgt*, side wall angle *SWA*, and period pitch. Dimensions of the structural parameters obtained from Fig. 2 are *TCD* = 353nm, *Hgt* = 472nm, and *SWA* = 80°. In the following experiments, structural parameters of the Si grating that need to be extracted include TCD, Hgt, and SWA, while the grating period is fixed at its nominal dimension, i.e., *pitch* = 800 nm.

3.2 Result and discussion

In the experiments, the spectral range is from 200 to 800nm with an increment of 5nm, the incident angle is fixed to 65 deg and the azimuthal angle is varied from 0 to 90 deg with a step of 5 deg. When applying the RCWA to calculate the Mueller matrices, the number of retained orders in the truncated Fourier series is 12, and the Si grating as shown in Fig. 2 is sliced into 15 layers along the vertical direction.

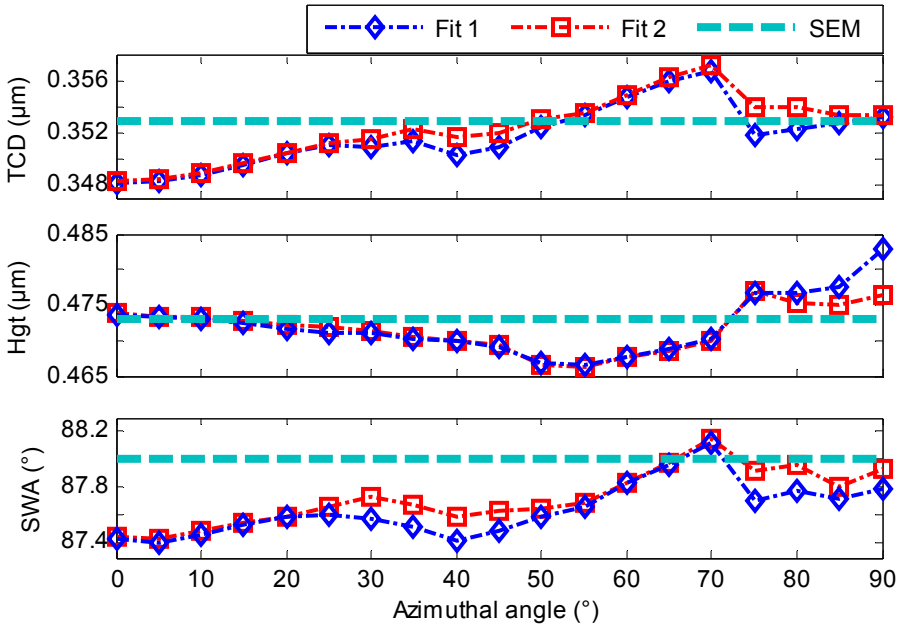

Figure 3. Comparison of structure parameters measured by SEM and extracted from the measured Mueller matrices with and without the polar decomposition approach. The 'Fit 1' represents the structure parameters extracted from the original measured Mueller matrices directly and the 'Fit 2' stands for the structure parameters extracted from the retarder and diattenuator matrices by performing the polar decomposition method.

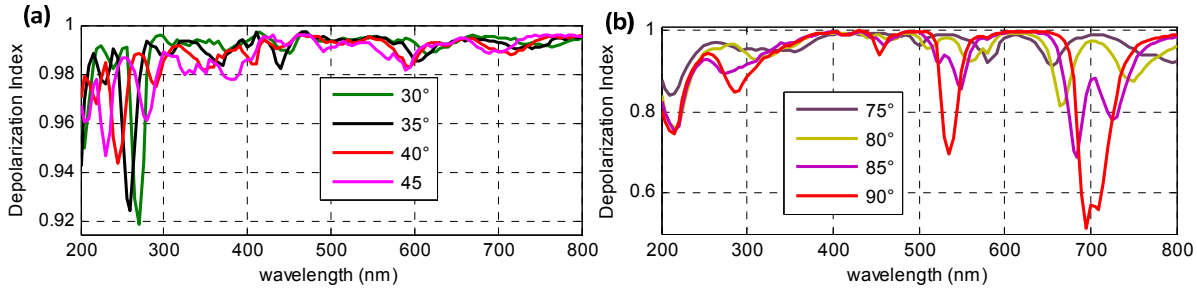

Figure 4. Depolarization Index of the Mueller matrix at the azimuthal angle of (a) 30°-45° and (b) 75°-90°.

The measured Mueller matrix spectra are first used to fit the calculated Mueller matrices, and the extracted structure parameters of the Si grating are shown in Fig. 3 as Fit 1. And then, the measured Mueller matrices are decomposed by the polar decomposition (2a). According to the proposed method, the retarder matrices and the diattenuator matrices are used to extract the structure parameters and results are shown in Fig.3. According to Fig. 3, we observed that the both

fitting results show a good agreement to the SEM results. However, the structure parameters extracted from the decomposed matrices are much closer to the SEM results over the azimuthal angle from 30 to 45 deg and 75 to 90 deg, while the two fitting results are nearly the same over the azimuthal angle from 0 to 25 deg and 50 to 70 deg. We calculated the depolarization indices of the measured Mueller matrices, and the DI spectra over the azimuthal angle from 30 to 45 deg and from 75 to 90 deg are shown in Fig. 4 (a) and (b), respectively. As can be observed, obvious depolarization effects are introduced in the Mueller matrix spectra over these azimuthal angle ranges. This observation means that, the proposed decomposition method gives access to a higher accuracy in the Si grating metrology in case depolarization effects are introduced in the Mueller matrix measurement. Figure 5 and 6 depict examples of the retarder matrices and diattenuator matrices obtained by the polar decomposition of the measured and the calculated Mueller matrices for the investigated Si grating at the azimuthal angle of 30° and incidence angle of 65°.

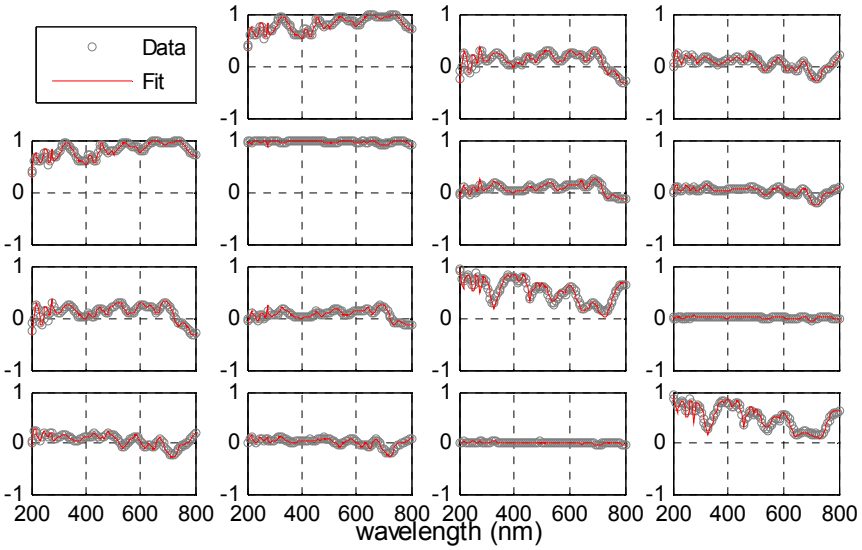

Figure 5. Example of the diattenuator matrix spectra decomposed from the measured (gray dot) and calculated (red solid lines) Mueller matrices for the investigated Si grating at the azimuthal angle of 30° and incidence angle of 65°.

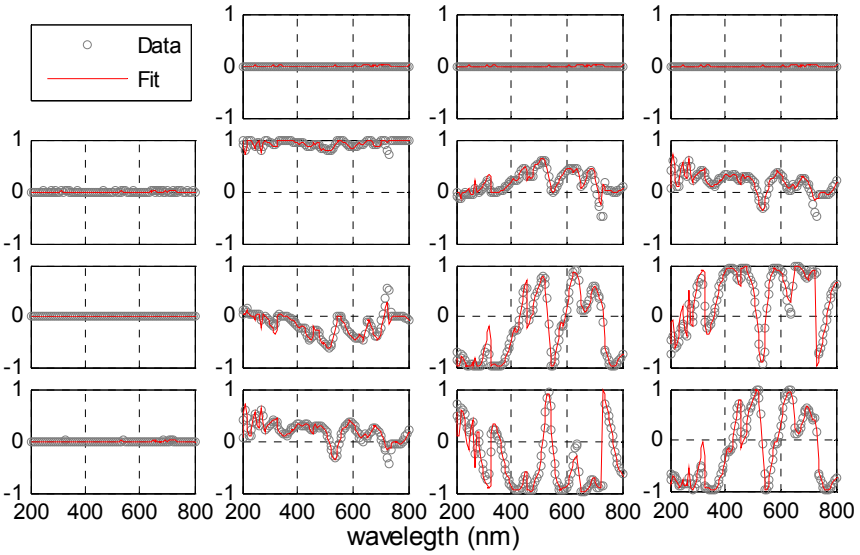

Figure 6. Example of the retarder matrix spectra decomposed from the measured (gray dot) and calculated (red solid lines) Mueller matrices for the investigated Si grating at the azimuthal angle of 30° and incidence angle of 65°.

4. CONCLUSIONS

Depolarization effects introduced in the Mueller matrix measurement may lead to accuracy loss in the nanostructure

metrology. We applied the polar decomposition to separate the depolarization effects. When the depolarization effects are mainly induced by the MME system, these effects will be only reflected in the depolarizer matrix. Therefore, the other two matrices, namely diattenuator matrix and retarder matrix, are used to extract the structure parameters of the nanostructure sample. Experiments performed on a silicon grating with an in-house developed dual rotating-compensator Mueller matrix ellipsometer have demonstrated the validity of the proposed method.

ACKNOWLEDGMENT

This work was funded by the National Natural Science Foundation of China (Grant Nos. 51475191 and 51405172), the National Instrument Development Specific Project of China (Grant No. 2011YQ160002), and the Program for Changjiang Scholars and Innovative Research Team in University of China (Grant No. IRT13017).

REFERENCES

[1] R.M.A. Azzam, and N.M. Bashara, [Ellipsometry and Polarized Light], North-Holland, Netherland, 1977.
[2] X. Niu, N. Jakatdar, J. Bao, and C. Spanos, "Specular spectroscopic scatterometry," IEEE Trans. Semicond. Manuf. **14**(2), 97-111 (2001).
[3] H. T. Huang, W. Kong, and F. L. Terry, "Normal-incidence spectroscopic ellipsometry for critical dimension monitoring," Appl. Phys. Lett. **78**(25), 3983-2985 (2001).
[4] H.T. Huang, and F.L. Terry Jr., "Spectroscopic ellipsometry and reflectometry from gratings (scatterometry) for critical dimension measurement and in situ, real-time process monitoring," Thin Solid Films 455, 828-836 (2004).
[5] H.J. Patrick, T.A. Germer, Y.F. Ding, H.W. Ro, L.J. Richter, and C.L. Soles, "Scatterometry for in situ measurement of pattern reflow in nanoimprinted polymers," Appl. Phys. Lett. **93**(23), 233105 (2008).
[6] M.G. Faruk, S. Zangooie, M. Angyal, D.K. Watts, M. Sendelbach, L. Economikos, P. Herrera, and R.Wilkins, "Enabling scatterometry as an in-line measurement technique for 32 nm BEOL application," IEEE Trans. Semicond. Manuf. **24**(4), 499 (2011).
[7] S. Y. Liu, X. G. Chen, and C. W. Zhang, " Development of a broadband Mueller matrix ellipsometer as a powerful tool for nanostructure metrology," Thin Solid Films (2015), http://dx.doi.org/10.1016/j.tsf.2015.02.006
[8] T. A. Germer, and H. J. Patrick, "Effect of bandwidth and numerical aperture in optical scatterometry," Proc. SPIE 7638, 76381F (2010).
[9] X. G. Chen, C. W. Zhang, and S. Y. Liu, " Depolarization effects from nanoimprinted grating structures as measured by Mueller matrix polarimetry," Appl. Phys. Lett. **103**(15), 151605 (2013)
[10] W. Q. Li, S. Y. Liu, C. W. Zhang, X. G. Chen, and H. G. Gu, "Correction on the effect of numerical aperture in optical scatterometry," Proc. SPIE **8916**, 89162l (2013).
[11] M. G. Moharam, E. B. Grann, D. A. Pommet, and T. K. Gaylord, "Formulation for stable and efficient implementation of the rigorous coupled wave analysis of binary gratings," J. Opt. Soc. Am. A **12**(5), 1068-1076 (1995).
[12] L. Li, "Use of Fourier series in the analysis of discontinuous periodic structures," J. Opt. Soc. Am. A **13**(9), 1870-1876 (1996).
[13] S. Y. Liu, Y. Ma, X. G. Chen, and C. W. Zhang, "Estimation of the convergence order of rigorous coupled-wave analysis for binary gratings in optical critical dimension metrology," Opt. Eng. **51**(8), 081504 (2012).
[14] H. Ichikawa, "Electromagnetic analysis of diffraction gratings by the finite-difference time-domain method," J. Opt. Soc. Am. A **15**(1), 152-157 (1998).
[15] H. Gross, R. Model, M. Bär, M. Wurm, B. Bodermann, and A. Rathsfeld, "Mathematical modelling of indirect measurements in scatterometry," Measurement **39**(9), 782-794 (2008).
[16] J. Pomplun, and F. Schmidt, "Accelerated a posterior error estimation for the reduced basis method with application to 3D electromagnetic scattering problems," SIAM J. Sci. Comput. **32**, 498-520 (2010).
[17] S. Y. Lu, and R. A. Chipman, "Interpretation of Mueller matrices based on polar decomposition"J. Opt. Soc. Am. A **13**(5), 1106-1113 (1996).
[18] J. Morio, and F. Goudail, "Influence of the order of diattenuator, retarder, and polarizer in polar decomposition of Mueller matrices," Opt. Lett. **29**(21), 2234-2236 (2004).
[19] R. Ossikovski, A. De Martino, and S. Guyot, "Forward and reverse product decompositions of depolarizing Mueller matrices," Opt. Lett. **32**(6), 689-671 (2007).

[20] J. J. Gil, and E. Bernabeu, "Depolarization and polarization indices of an optical system," Opt. Acta (Lond.) **33**(2), 185–189 (1986).
[21] H. Fujiwara, [Spectroscopic Ellipsometry: Principles and Applications], Wiley, West Sussex, 2007.
[22] R. W. Collins, and J. Koh, "Dual rotating-compensator multichannel ellipsometer: instrument design for real-time Mueller matrix spectroscopy of surfaces and films," J. Opt. Soc. Am. A **16**(8), 1997-2006 (1999).
[23] C. M. Herzinger, B. Johs, W. A. McGahan, J. A. Woollam, and W. Paulson, "Ellipsometric determination of optical constants for silicon and thermally grown silicon dioxide via a multi-sample, multi-wavelength, multi-angle investigation," J. Appl. Phys. **83**(6), 3323–3336 (1998).